

On the Dirac Structure of the Nucleon Selfenergy in Nuclear Matter

A. Trasobares, A. Polls, A. Ramos

*Departament d'Estructura i Constituents de la Matèria
Universitat de Barcelona, E-08028 Barcelona, Spain*

H. Mütter

*Institut für Theoretische Physik,
Universität Tübingen, D-72076 Tübingen, Germany*

Abstract

The relativistic structure of the self-energy of a nucleon in nuclear matter is investigated including the imaginary and real components which arise from the terms of first and second order in the NN interaction. A parameterized form of Brueckner G matrix is used for the NN interaction. The effects of the terms beyond the DBHF approximation on quasiparticle energies and the optical potential for nucleon-nucleus scattering are discussed.

1 Introduction

During the last few years the attempts to derive the ground-state properties of nuclear systems from a realistic nucleon-nucleon (NN) interaction, have been promoted very much by the understanding that relativistic effects may be non-negligible in such investigations. These ideas were originally developed within the various versions of the phenomenological Walecka model[1]. The Dirac structure of the NN interaction with a strong repulsive component originating from the exchange of the ω vector meson and an attractive component of medium range described in terms of a scalar meson (σ) leads to a self-energy of the nucleon in the nuclear medium which contains a large scalar component Σ^s and a large time like vector component Σ^0 . These two components compensate each other to a large extent if one calculates the single-particle energy. This leads to the well known fact that the binding-energy of nuclei are very small as compared to the rest mass of the nucleon M , a fact which has often been used to argue that relativistic effects should be small in the many-body problem of nuclear physics. The individual components of the self-energy Σ^s are of the order of the nucleon rest mass (typically one third of M). Therefore the structure of the Dirac spinors in the nuclear medium is modified to quite some extent as compared to the Dirac spinor for a free nucleon. This medium dependence of the Dirac spinors, which affects the evaluation of the NN interaction in the medium, leads to a saturation mechanism for nuclear matter.

These more or less empirical models received support from calculations, which start from a realistic One-Boson-Exchange model of the NN interaction[2]. In this context realistic NN interaction means that the parameters contained in these models are adjusted to describe the experimental data of free NN scattering. Using such a realistic NN interaction in a many-body calculation of the Dirac-Brueckner-Hartree-Fock (DBHF) type, results were obtained for the saturation point of nuclear matter which were in quite a good agreement with the empirical saturation point[3, 4]. Such a DBHF calculation accounts for the effect of correlations on the level of the BHF approximation, i.e. the lowest order in the hole line expansion, and allows for the relativistic effects which we just outlined. This success of the relativistic features contained in the DBHF approach could be a solution of an old problem: the so-called Coester band phenomenon[5], which stands for the fact that many-body calculations based on various realistic models of the NN interaction lead to predictions for the saturation point of nuclear matter, which either fail to yield enough binding or predict a saturation density twice as large as the empirical value.

Such a Coester band can also be observed in non-relativistic studies of finite nuclei[6]. Therefore it was quite obvious that attempts have been made to include the relativistic features also in DBHF calculations of finite nuclei. Indeed the inclusion of relativistic effects gave a substantial improvement in the calculated binding energies and radii of finite nuclei[7, 8]. However, there remains still a discrepancy between the DBHF results and the experimental values.

On the other hand it was observed that an extension of the non-relativistic BHF approach to a definition of the nucleon self-energy which accounts in a symmetric way not only for the particle-particle ladders included in the Brueckner G -matrix but also for the corresponding hole-hole scattering term may lead to a larger binding energy and a larger radius than obtained in the BHF approach[9]. A similar feature, moving the saturation point away from the Coester band by including hole-hole scattering terms, has also been observed in particle-particle hole-hole RPA calculation of nuclear matter[10, 11]. Taking a very optimistic point of view one may argue that the combination of relativistic effects and hole-hole scattering terms may lead to an improved microscopic understanding of groundstate properties of nuclear systems.

In the work presented here we would like to investigate the effects of particle-particle and hole-hole scattering terms on the relativistic structure of the nucleon self-energy. For that purpose we consider the nucleon self-energy defined with all terms of first and second order in the NN interaction (see Fig. 1). In contrast to earlier investigations[12, 13, 14, 15] we evaluate the imaginary contributions to the nucleon self-energy allowing for all possible combinations of momentum \mathbf{k} and energy k^0 . Therefore we can use dispersion relations to evaluate also the real part of the second order diagrams. We investigate in detail the effect of these higher order diagrams on the Dirac structure of the self-energy. Furthermore we derive from this relativistic self-energy an optical potential to be used in a Schrödinger equation for nucleon-nucleus scattering.

The technical details for the calculation of the imaginary components in the self-energy are presented in section 2. The dispersion relations used to evaluate the corresponding real components are given in section 3. That section also contains a detailed discussion of the results. The main conclusions are summarized in the final section.

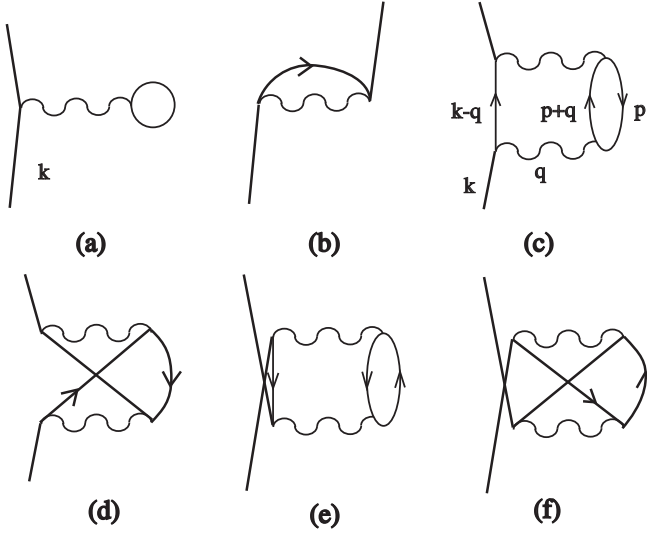


Figure 1: Graphical representation of the Hartree (a), Fock (b), 2p1h direct (c), 2p1h exchange (d), 2h1p direct (e) and 2h1p exchange (f) contributions to the self-energy of the nucleon. The momenta labelling the various contractions in (c) correspond to the nomenclature used in (15)

2 Imaginary part of the nucleon self-energy

The physical system of neutron or nuclear matter is, by definition, translational as well as rotational invariant. Furthermore it is also assumed to be invariant under parity and time reversal. In general, under these conditions, the nucleon self-energy can be written¹ as [1]:

$$\Sigma(\mathbf{k}) = \Sigma^s(\mathbf{k}) - \gamma_0 \Sigma^0(\mathbf{k}) + \boldsymbol{\gamma} \cdot \mathbf{k} \Sigma^v(\mathbf{k}) \quad (1)$$

where the functions Σ^r ($r = s, 0, v$) can be projected out by taking the appropriate traces:

$$\Sigma^s = \frac{1}{4} \text{Tr}[\Sigma] \quad (2)$$

$$\Sigma^0 = \frac{-1}{4} \text{Tr}[\gamma_0 \Sigma] \quad (3)$$

$$\Sigma^v = \frac{-1}{4\mathbf{k}^2} \text{Tr}[\boldsymbol{\gamma} \cdot \mathbf{k} \Sigma] \quad (4)$$

As mentioned in the introduction, in this work we want to go beyond the usual Hartree-Fock approximation to the self-energy, visualized by the diagrams a and b of Fig. 1, and pay special attention to the 2hole-1particle (2h1p) and 2particle-1hole (2p1h) diagrams displayed in Figs. 1c, 1d, 1e and 1f. Therefore, the different components of the self-energy are complex functions and, in general, we will write them as:

$$\Sigma^r = V^r + iW^r \quad (5)$$

¹Notation: within formulæ we shall use roman type (p, q, \dots) for 4-vectors, boldface type ($\mathbf{p}, \mathbf{q}, \dots$) for 3-vectors and normal math italic type (p, q, \dots) for the norm of 3-vectors.

Previous works have focused on the imaginary part of the self-energy at the on-shell energy of the propagating nucleon. In Ref. [12] the 2p1h and 2h1p direct contributions were studied, while the work of Ref. [14] considered also the Fock-exchange terms. This study, however, was restricted to the on-shell 2h1p contributions.

In the present work we extend these calculations and evaluate the direct and exchange terms for both 2h1p and 2p1h contributions to the nucleon self-energy considering off-shell effects, i.e. investigating the self-energy $\Sigma(k_0, \mathbf{k})$ for all combinations of energy k_0 and momentum \mathbf{k} . In a first step we calculate the imaginary part of the self-energy, as described below, from which we later obtain the real part by means of a dispersion relation.

The nucleon-nucleon interaction is derived from a G -matrix evaluated within the Dirac-Brueckner-Hartree-Fock approach. This G -matrix is parameterized in terms of an exchange of effective σ and ω mesons[7, 16]. The starting point of our discussion will be the Hartree-Fock (HF) approach. Therefore, and for the sake of simplifying the notation, we will define the following effective quantities in terms of the Hartree-Fock components of the self-energy:

$$M^*(\mathbf{k}) = M + \Sigma_{HF}^s(\mathbf{k}) \quad (6)$$

$$\mathbf{k}^* = \mathbf{k}(1 + \Sigma_{HF}^v(\mathbf{k})) \quad (7)$$

$$E^*(\mathbf{k}) = \sqrt{\mathbf{k}^{*2} + M^{*2}} \quad (8)$$

$$k^* \equiv (k_0^*, \mathbf{k}^*) = (k_0 + \Sigma_{HF}^0(\mathbf{k}), \mathbf{k}^*) \quad (9)$$

$$\epsilon_{HF}(\mathbf{k}) = E^*(\mathbf{k}) - \Sigma_{HF}^0(\mathbf{k}) \quad (10)$$

The nucleon HF propagator is then

$$G(\mathbf{k}) = \frac{\mathbf{k}^* + M^*(\mathbf{k})}{2E^*(\mathbf{k})} g(\mathbf{k}) \quad (11)$$

where

$$g(\mathbf{k}) = \frac{\theta(E^*(\mathbf{k}) - E_F^*)}{k_0^* - E^*(\mathbf{k}) + i\eta} + \frac{\theta(E_F^* - E^*(\mathbf{k}))}{k_0^* - E^*(\mathbf{k}) - i\eta} - \frac{1}{k_0^* + E^*(\mathbf{k}) - i\eta} \quad (12)$$

with $E_F^* = \sqrt{k_F^{*2} + M^{*2}}$. In eq. (12) we will disregard the last term, which is the anti-nucleon contribution. This is quite reasonable due to two reasons. First of all, the production of fermion anti-fermion pairs should be negligible at the energy scales of interest and secondly the pair production is inhibited in high density matter [12, 13]. In the actual calculations we set $\Sigma_{HF}^v = 0$ and disregard the momentum dependence of Σ_{HF}^s and Σ_{HF}^0 for which we take their values at the Fermi momentum k_F . This approximation relies on the weak momentum dependence of the Hartree-Fock self-energies [1]. In this way, M^* acquires a fixed value, $\mathbf{k}^* = \mathbf{k}$, and the only effective quantity that depends on the nucleon momentum is E_k^* , which from now on will be labelled with a subindex. It is also useful to split up the fermion-propagator into a particle and a hole term and consider explicitly all terms of Fig. 1 by taking the following prescriptions for the nucleon propagators in the diagrams:

$$\text{Particle line} : iG_p(\mathbf{k}) = i \frac{\mathbf{k}^* + M^*}{2E_k^*} g_p(\mathbf{k}) \quad (13)$$

$$\text{Hole line} : iG_h(\mathbf{k}) = i \frac{\mathbf{k}^* + M^*}{2E_k^*} g_h(\mathbf{k}) , \quad (14)$$

where the g -functions for particle and hole states are defined as:

$$g_p(k) = \frac{\theta(E_k^* - E_F)}{k_0^* - E_k^* + i\eta}$$

$$g_h(k) = \frac{\theta(E_F - E_k^*)}{k_0^* - E_k^* - i\eta}$$

These g -functions are formally similar to the non-relativistic HF nucleon propagators. Therefore, applying the standard Feynman rules together with the prescriptions of Eqs. (13) and (14), we obtain a general expression for the 2p1h contribution

$$i\Sigma_{X;ab}(k_0, k) = i \int \frac{d^4q}{(2\pi)^4} \frac{d^4p^*}{(2\pi)^4} \mathcal{M}_{X;ab}(k, p, q) g_p(p+q) g_h(p) g_p(k-q) \quad (15)$$

while the formula for the 2h1p state is identical to the above except for the exchange of the p and h subscripts in the g -functions. The subscript X stands for D (direct) and E (exchange) diagrams, while a and b stand for the different meson types.

The function $\mathcal{M}_{X;ab}(k, p, q)$ contains, basically, the Dirac structure of the interaction and, for direct terms, it has the general form,

$$\mathcal{M}_{D;ab}(k, p, q) = \frac{-\lambda_I g_a^2 g_b^2}{8E_p^* E_{p+q}^* E_{k-q}^*} \Gamma_b(q) \Delta_b(q) Tr[\Gamma_b(q) (\not{p}^* + \not{q}^* + M^*) \Gamma_a(q) (\not{p}^* + M^*)] (\not{k}^* - \not{q}^* + M^*) \Delta_a(q) \Gamma_a(q) \quad (16)$$

The constant λ_I is the isospin degeneracy and comes from the loop trace, g_a and g_b are the meson-nucleon coupling constants. The meson-nucleon vertices are denoted by Γ and meson propagators by Δ . A form factor of the type $F(q) = \frac{\Lambda^2}{\Lambda^2 - q^2}$, with a typical cut-off mass of $\Lambda = 1500$ MeV, has been attached to each vertex. This is equivalent to modifying the meson propagators in the following way:

$$\Delta_a(q) \longrightarrow \Delta_a(q) F^2(q) \quad (17)$$

Note as well the minus sign that comes from the fermion loop. For exchange terms one can write:

$$\mathcal{M}_{E;ab}(k, p, q) = \frac{g_a^2 g_b^2}{8E_p^* E_{p+q}^* E_{k-q}^*} \Gamma_b(k-q-p) \Delta_b(k-q-p) (\not{p}^* + \not{q}^* + M^*) \Gamma_a(q) (\not{p}^* + M^*) \Gamma_b(k-q-p) (\not{k}^* - \not{q}^* + M^*) \Delta_a(q) \Gamma_a(q) \quad (18)$$

The imaginary part of the self-energy is obtained as:

$$W_{X;ab}(k_0, k) = 4\pi^3 \int \frac{d^4q}{(2\pi)^4} \frac{d^4p^*}{(2\pi)^4} \mathcal{M}_{X;ab}(k, p, q) \Theta(k, p, q) \quad (19)$$

Where, for 2p1h, the factor Θ has the following form:

$$\Theta(k, p, q) = \theta(E_F - p_0^*) \theta(k_0^* - q_0 - E_F^*) \theta(p_0^* + q_0 - E_F^*) \delta(p_0^* - E_p^*) \delta(p_0^* + q_0 - E_{p+q}^*) \delta(k_0^* - q_0 - E_{k-q}^*) \quad (20)$$

and, for 2h1p:

$$\begin{aligned} \Theta(\mathbf{k}, \mathbf{p}, \mathbf{q}) = & -\theta(p_0^* - E_F^*)\theta(E_F^* - k_0^* + q_0)\theta(E_F^* - p_0^* - q_0) \\ & \delta(p_0^* - E_p^*)\delta(p_0^* + q_0 - E_{\mathbf{p}+\mathbf{q}}^*)\delta(k_0^* - q_0 - E_{\mathbf{k}-\mathbf{q}}^*) \end{aligned} \quad (21)$$

One can now use the step functions to define the boundaries for the integrations over dq_0 and dp_0 . Working in spherical coordinates we can automatically perform one of the axial integrations (say over the axial \mathbf{q} -angle). By rewriting the first δ -function in terms of the 3-momentum variable, the dp integration can be easily performed. After that we obtain, for the 2p1h diagrams,

$$\begin{aligned} W_{X;ab}(k_0, k) = & \frac{1}{2(2\pi)^4} \int_0^{k_0^* - E_F^*} dq_0 \int dq \, q^2 \, d(\cos \theta_q) \int_{\bar{p}_0}^{E_F^*} dp_0^* \, p \int d\varphi_p \, d(\cos \theta_p) \\ & \mathcal{M}_{X;ab}(\mathbf{k}, \mathbf{p}, \mathbf{q}) \, E_p^* \, \delta(p_0^* + q_0 - E_{\mathbf{p}+\mathbf{q}}^*) \delta(k_0^* - q_0 - E_{\mathbf{k}-\mathbf{q}}^*) \end{aligned} \quad (22)$$

Where, p takes the value $p = \sqrt{p_0^{*2} - M^{*2}}$, and

$$\bar{p}_0 = \max(E_F^* - q_0, M^*). \quad (23)$$

For the 2h1p contribution one obtains a similar expression up to an overall minus sign. The polar integration over the angle θ_q between \mathbf{q} and the external momentum \mathbf{k} (taken along the z-axis) is readily performed by using the delta function

$$\delta(k_0^* - q_0 - E_{\mathbf{k}-\mathbf{q}}^*) \equiv \frac{E_{\mathbf{k}-\mathbf{q}}^*}{kq} \delta(\cos \theta_{kq} - \frac{2k_0^*q_0 - q^2 + M^{*2} - k^{*2}}{2kq}),$$

which, in order to keep $|\cos \theta_{kq}| < 1$, imposes the following constraints to the q variable:

$$q_- \leq q \leq q_+$$

where:

$$q_{\pm} = |p \pm \sqrt{(k_0^* - q_0)^2 - M^{*2}}|.$$

The integration over the polar angle θ_p can also be performed very easily by referring the two angular variables of the momentum \mathbf{p} (ϕ_p, θ_p) to a reference frame in which \mathbf{q} acts as the z-axis and using the remaining δ -function

$$\delta(p_0^* + q_0 - E_{\mathbf{p}+\mathbf{q}}^*) \equiv \frac{E_{\mathbf{p}+\mathbf{q}}^*}{pq} \delta(\cos \theta_{pq} - \frac{2p_0^*q_0 + q^2}{2pq}).$$

The requirement that the absolute value of the cosine must be less than one puts restrictions to the values of p_0^* , similar to those obtained for q , but more complicated to be implemented analytically due to the two different sign possibilities for q^2 . For this reason, we have taken care of the restrictions over p_0^* numerically through an explicit step function inside the integral.

After all these considerations we can write our final expression for the imaginary part of the self-energy. For the 2p1h state we have:

$$\begin{aligned} W_{X;ab}(k_0, k) = & \frac{1}{2(2\pi)^4 k} \int_0^{k_0^* - E_F^*} dq_0 \int_{q_-}^{q_+} dq \int_{\bar{p}_0}^{E_F^*} dp_0^* \, \theta(1 - \left[\frac{2p_0^*q_0 + q^2}{2pq} \right]^2) \int_0^{2\pi} d\varphi_p \\ & \tilde{\mathcal{M}}_{X;ab}(k_0^*, k, p_0^*, q_0, q, \varphi_p), \end{aligned} \quad (24)$$

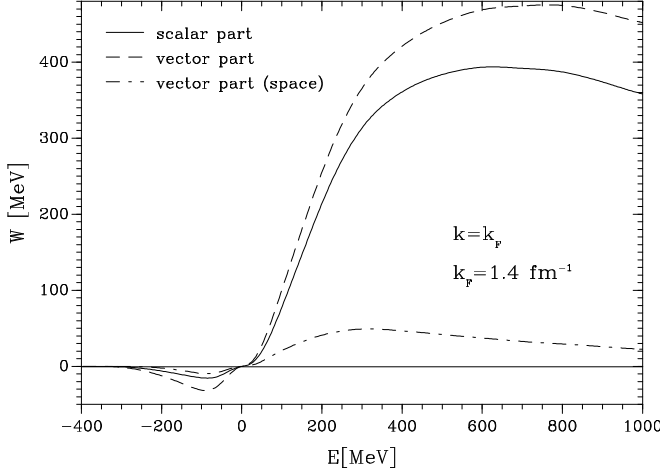


Figure 2: Imaginary part of the self-energy calculated for a fixed momentum $k = k_F = 1.4 \text{ fm}^{-1}$ as a function of the energy variable, which is normalized such that it is zero at the Fermi energy. Results are displayed for the scalar part (W^s , solid line), the time-like vector part (W^0 , dashed line) and the space-like vector component (W^v , dashed dotted line)

and for the 2h1p state:

$$W_{X;ab}(k_0, k) = \frac{-1}{2(2\pi)^4 k} \int_{k_0^* - E_F^*}^0 dq_0 \int_{q_-}^{q_+} dq \int_{E_F^*}^{E_F^* - q_0} dp_0^* \theta\left(1 - \left[\frac{2p_0^* q_0 + q^2}{2pq}\right]^2\right) \int_0^{2\pi} d\varphi_p \tilde{\mathcal{M}}_{X;ab}(k_0^*, k, p_0^*, q_0, q, \varphi_p), \quad (25)$$

where it is understood that $\tilde{\mathcal{M}}$ does not contain the energies in the denominators of Eqs. (16) and (18) because they have canceled out with the energy factors that appeared on rewriting the δ -functions.

3 Results and Discussion

In the first part of this section we will concentrate the discussion of results on the example of nuclear matter at a density close to the saturation density, in particular we will consider a Fermi momentum k_F of 1.4 fm^{-1} . We are going to discuss the contribution of the diagrams of second order in the NN interaction to the various components of the imaginary part in the nucleon self-energy. The NN interaction is described in terms of the exchange of an effective scalar, σ , meson and an effective vector, ω , meson. The masses of these mesons are fixed to the masses of the corresponding mesons in a realistic meson exchange model of the NN interaction ($m_\sigma = 550 \text{ MeV}$, $m_\omega = 782.6 \text{ MeV}$), while the effective coupling constants have been adjusted [7] such that a Dirac-Hartree-Fock calculation of nuclear matter at $k_F = 1.4 \text{ fm}^{-1}$ using these constants would reproduce the results for single-particle energies and the binding energy obtained in a Dirac-Brueckner-Hartree-Fock (DBHF) calculation employing Bonn A

NN potential[2]. This Dirac-Hartree-Fock parameterization of the DBHF results yields at this density coupling constants of $g_\sigma=8.536$ and $g_\omega=9.536$ for the σ and the ω meson, respectively[7]. The single-particle Green function G of eq.(11) for the propagation of the intermediate states is also defined employing the results of this DBHF calculation. This means that we consider a HF self-energy defined in terms of

$$\begin{aligned}\Sigma_{HF}^s &= -374.9 \text{ MeV} \\ \Sigma_{HF}^0 &= -289.8 \text{ MeV}.\end{aligned}\tag{26}$$

As a first example we show in Fig. 2 the imaginary part of the self-energy calculated for nucleons with a momentum fixed to $k = k_F = 1.4 \text{ fm}^{-1}$ as a function of the energy. Note that the energy variable in this figure is normalized such that an energy zero corresponds to the Fermi energy $\epsilon_F = \epsilon_{HF}(k_F)$ as defined in (10). Results are displayed for the scalar component, $\text{Imag}\Sigma^s = W^s$, the time-like vector component, $\text{Imag}\Sigma^0 = W^0$, and the space-like vector component, $k\text{Imag}\Sigma^v = W^v$. All these components are negative at energies below the Fermi energy and positive for those above. They are much larger at positive energies, reflecting the fact that the phase space of 2 particle 1 hole (2p1h) states with this momentum k is considerably larger than the corresponding phase space of 2 hole 1 particle states (2h1p). The scalar and time-like vector part are of similar size and exhibit the same sign. Using our notation this means that these contributions cancel each other to a large extent in calculating the expectation value for a Dirac spinor u representing a nucleon, i.e. a solution of the Dirac equation at positive energy:

$$\bar{u}(k)\text{Imag}\Sigma(k_0, \mathbf{k})u(k) = -W^0(k_0, \mathbf{k}) + \frac{M^*}{E^*}W^s(k_0, \mathbf{k}) + \frac{\tilde{\mathbf{k}}\mathbf{k}^*}{E^*}\tag{27}$$

using the definition

$$\tilde{\mathbf{k}} = \mathbf{k}W^v(k_0, \mathbf{k})\tag{28}$$

and E^* , M^* , \mathbf{k}^* as defined in eqs.(6) - (8). The Dirac spinors u are normalized such that $u^\dagger u = 1$. As the absolute value of W^0 is always larger than the absolute value of W^s at the same energy, this expectation value, which is roughly proportional to $W^s - W^0$, shall be positive at energies below the Fermi energy and negative above, as it is the case for the imaginary part of the self-energy calculated within a non-relativistic frame. The space-component of the vector part, $\tilde{\mathbf{k}}$, is significantly smaller than the other terms. This difference, however, is not as large as one finds, e.g. in the real part of the self-energy calculated within the Dirac-Hartree-Fock approach. Similar results are obtained for other momenta and nuclear densities.

From the 2h1p contribution to the imaginary part, i.e. the one at energies below the Fermi energy E_F^* one can determine the corresponding contribution to the real part by applying the dispersion relation

$$\begin{aligned}\Delta V_{2h1p}^\alpha(\omega, k) &= \text{Real}\Delta\Sigma_{2h1p}^\alpha(\omega, k) \\ &= \frac{P}{\pi} \int_{-\infty}^0 d\omega' \frac{\text{Imag}\Sigma_{2h1p}^\alpha(\omega', k)}{\omega - \omega'},\end{aligned}\tag{29}$$

where the P is used to indicate the principle value integral and the index α represents s , 0 , and v , referring to the scalar and vector components of Σ . Note that here and in

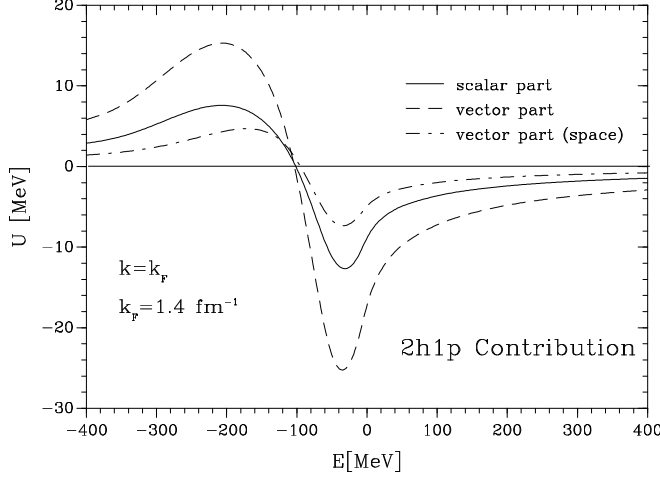


Figure 3: Real part of the 2h1p contribution to the self-energy for a fixed momentum as a function of energy. For further details see Fig. 2.

the following the energy variables ω are redefined such that $\omega = 0$ corresponds to the Fermi energy $k_0 = \epsilon_F$. Typical examples for the real part of the 2h1p contribution to the self-energy are displayed in Fig. 3. The energy dependence of these terms, can easily be understood from the energy dependence of the imaginary part, shown in Fig. 2, and the dispersion relation of eq.(29). All three contributions are negative for energies between -100 MeV and the Fermi energy, which are typical energies for quasihole states, as well as for positive energies, i.e. particle states with energies above the Fermi energy ϵ_F . As the absolute value of the time-like vector component $\text{Real}\Delta\Sigma_{2h1p}^0$ (dashed line) is consistently larger than the corresponding scalar component (solid line), we obtain a repulsive contribution to the quasiparticle energy, arising from this 2h1p term from energies starting around -100 MeV below the Fermi energy up to infinity. This repulsive contribution is largest for quasihole states with energies below ϵ_F and will decrease for energies above ϵ_F with increasing energy. It should be noted that the space-like vector component exhibits a sizable contribution.

The real part of the 2p1h contribution to the nucleon self-energy can be calculated from the corresponding imaginary part by a dispersion relation rather similar to eq.(29)

$$\text{Real}\Delta\Sigma_{2p1h}^\alpha(\omega, k) = -\frac{P}{\pi} \int_0^\infty d\omega' \frac{\text{Imag}\Sigma_{2p1h}^\alpha(\omega', k)}{\omega - \omega'}. \quad (30)$$

We already discussed above that the 2p1h states lead to larger contributions to the imaginary part than the 2h1p terms. Therefore it is clear that the 2p1h contributions to the real part of the self-energy are significantly larger than those originating from 2h1p terms. This can be seen from Fig. 4, which employs a scale which is about a factor 10 larger than the one used in Fig. 3 to visualize the 2h1p contributions.

In the energy range of interest all three terms are positive. This means that the 2p1h contribution to the scalar part of the self-energy Σ^s tends to compensate the negative Hartree-Fock contribution to this term originating mainly from the exchange of two correlated pions, which is parameterized in the realistic OBE potentials by means of

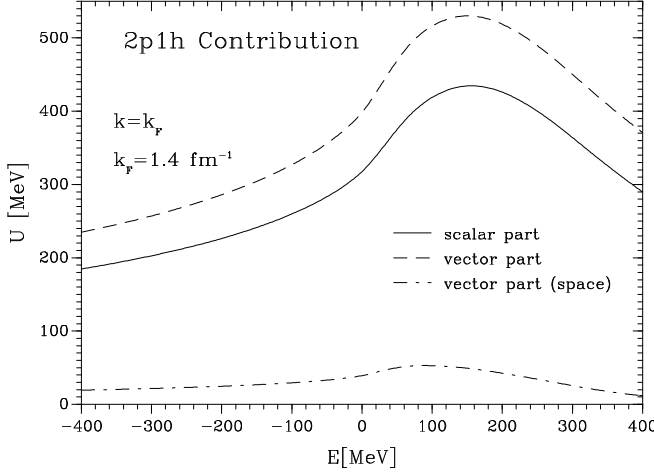


Figure 4: Real part of the 2p1h contribution to the self-energy for a fixed momentum as a function of energy. For further details see Fig. 2.

the σ meson exchange. A similar situation also arises in the case of the timelike vector component of the nucleon self-energy Σ^0 : The negative Hartree-Fock contribution to Σ^0 , which is mainly due to the exchange of the ω meson, is compensated to some extent by the 2p1h terms. This means that the 2p1h terms tend to reduce the Hartree-Fock contributions to the various terms in the self-energy while the 2h1p corrections yield contributions to Σ^s and Σ^0 with the same sign as the Hartree-Fock terms. Similar results are obtained for other momenta k .

Since, however, our Hartree-Fock approximation to the self-energy has already been extracted from a DBHF calculation, we are not allowed to simply add the real part of 2p1h contribution to the self-energy to the corresponding DBHF results. This would lead to a double counting of these 2p1h terms. Instead we use a subtracted dispersion relation defined by

$$\Delta V_{2p1h}^\alpha(\omega, k) = \text{Real} \Delta \Sigma_{2p1h}^\alpha(\omega, k) - \text{Real} \Delta \Sigma_{2p1h}^\alpha(\epsilon_{HF}(k) - \epsilon_F, k) \quad (31)$$

using the real contributions to the various terms α in the self-energy as defined in (30). With these definitions we now define a quasiparticle self-energy, which is real and energy dependent, to be

$$V_{qp}^\alpha(\omega, k) = \Sigma_{HF}^\alpha(k) + \Delta V_{2p1h}^\alpha(\omega, k) + \Delta V_{2h1p}^\alpha(\omega, k) \quad (32)$$

and we can determine a quasiparticle spinor

$$u_{qp}(\mathbf{k}) = \sqrt{\frac{E_{qp}^* + M_{qp}^*}{2E_{qp}^*}} \begin{pmatrix} 1 \\ \frac{\vec{\sigma} \cdot \mathbf{k}_{qp}^*}{E_{qp}^* + M_{qp}^*} \end{pmatrix} \quad (33)$$

with

$$\begin{aligned} M_{qp}^* &= M + V_{qp}^s(\omega_{qp}, k) \\ \mathbf{k}_{qp}^* &= \mathbf{k}(1 + V_{qp}^v(\omega_{qp}, k)) \end{aligned}$$

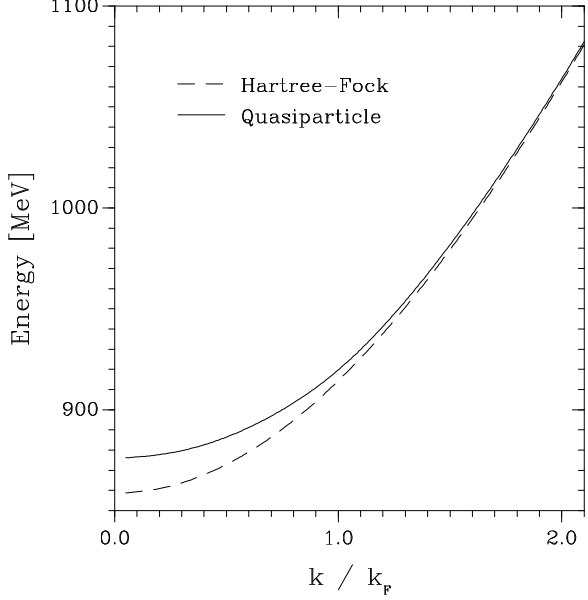


Figure 5: Results for the quasiparticle energy, calculated according to eq. (36), are compared to the corresponding energies calculated in the HF approximation for the self-energy (dashed line)

$$\begin{aligned} E_{qp}^* &= \sqrt{(\mathbf{k}_{qp}^*)^2 + (M_{qp}^*)^2} \\ \omega_{qp} &= E_{qp}^* - V_{qp}^0(\omega_{qp}, k) - \epsilon_F. \end{aligned} \quad (34)$$

This means that this spinor is an eigenstate of the Dirac equation

$$\left[(1 + V_{qp}^v) \vec{\alpha} \cdot \mathbf{k} + \gamma^0 (M + V_{qp}^s) - V_{qp}^0 \right] u_{qp} = \epsilon_{qp} u_{qp}, \quad (35)$$

which uses the self-energy V_{qp} of (32) calculated at the energy ω which corresponds to the quasiparticle energy defined by

$$\epsilon_{qp}(k) = E_{qp}^* - \Sigma_{qp}^0(\omega_{qp}, k). \quad (36)$$

If for the moment we ignore the 2h1p contribution, ΔV_{2h1p}^α , to the quasiparticle self-energy in (32), the subtraction defined in (31) ensures that the ΔV_{2p1h}^α terms vanish on-shell and the quasiparticle energy coincides with the HF energy, thus avoiding double counting. However, when the contribution of the 2h1p terms is taken into account, the self-consistent definition of the energy variable ω_{qp} gives rise to a non-vanishing correction due to energy dependence of the 2p1h terms.

Results for the quasiparticle energy are displayed in Fig. 5 for various momenta k . It can be seen that the inclusion of the 2h1p terms yields a significant reduction in the quasiparticle energy ϵ_{qp} as compared to the corresponding HF result. This reduction is as large as 17.5 MeV for momenta close to zero and reduces to values around 5.3 MeV for $k = k_F$ and becomes negligibly small around $k = 2k_F$. This repulsive effect of the 2h1p terms in the quasiparticle energy has been discussed already in context with Fig. 3. Such a large effect for the quasiparticle energy may indicate that the

2h1p terms may as well have some effect in the calculation of the total energy. For the calculation of the total energy, however, it is not sufficient to evaluate the quasiparticle energy, but one would need the whole spectral distribution of hole strength for states with momenta below and above the Fermi momentum[17].

It is one aim of our study to explore the effects of the Dirac structure of the nucleon self-energy, calculated beyond the mean field approximation, on the complex optical potential for nucleon-nucleus scattering. The Dirac equation reads now:

$$\left[(1 + \Sigma_{qp}^v) \vec{\alpha} \cdot \mathbf{k} + \gamma^0 (M + \Sigma_{qp}^s) - \Sigma_{qp}^0 \right] u_{qp} = \tilde{\epsilon}_{qp} u_{qp} \quad (37)$$

where the full complex self-energy is used. Real $\tilde{\epsilon}_{qp}$ solutions of eq. (37) involve complex values of \mathbf{k} . We take as approximate solutions of eq. (37) the values ϵ_{qp} determined from eq. (36). It is convenient to rewrite eq. (37) into a form which only contains an effective scalar \mathcal{V}^s and vector potential \mathcal{V}^0 [18]

$$\left[\vec{\alpha} \cdot \mathbf{k} + \gamma^0 (M + \mathcal{V}^s) - \mathcal{V}^0 \right] u_{qp} = \epsilon_{qp} u_{qp}$$

where

$$\begin{aligned} \mathcal{V}^s &= \frac{\Sigma_{qp}^s - M \Sigma_{qp}^v}{1 + \Sigma_{qp}^v}, \\ \mathcal{V}^0 &= \frac{\Sigma_{qp}^0 - \epsilon_{qp} \Sigma_{qp}^v}{1 + \Sigma_{qp}^v}. \end{aligned} \quad (38)$$

The self-energy terms Σ_{qp}^α have been calculated in the quasiparticle approach of (32) using the self-consistent relation between the three-momentum and the energy as defined in (34). This Dirac equation can be transformed into a Schrödinger-type equation for the large component of the Dirac spinor, leading to a complex and energy-dependent Schrödinger equivalent potential of the form

$$\mathcal{U} = \mathcal{V}^s - \frac{\epsilon_{qp}}{M} \mathcal{V}^0 + \frac{1}{2M} [(\mathcal{V}^s)^2 - (\mathcal{V}^0)^2]. \quad (39)$$

Results for the real part of the renormalized components \mathcal{V}^s and \mathcal{V}^0 are displayed in Fig. 6 as a function of the energy variable ω_{qp} , i.e. the quasiparticle energy ϵ_{qp} normalized such that the Fermi energy occurs at zero. For a comparison we also show the unrenormalized components V_{qp}^α . The difference between the solid and dashed line is a measure for the importance of the space-like vector component Σ^v of the self-energy. We find that this space like components yield a slight reduction of the absolute values for $\text{Real}\mathcal{V}$, which is of the order of 3 percent. Larger effects only occur at negative energies, below the Fermi energy, where the 2h1p contribution gets more important.

This figure also demonstrates that the energy-dependence of the various Dirac components in the real part of the self-energy remains weak, again with the exception of energies below ϵ_F . Also the deviations from the Hartree-Fock result, -375 MeV and -290 MeV for the scalar and vector parts, respectively, are not very pronounced. This can also be seen from the left part of Fig. 7, exhibiting the real part of the Schrödinger equivalent potential \mathcal{U} defined in (39). The results derived from the quasiparticle approximation (solid line) including the effects of the energy-dependence in the 2p1h and

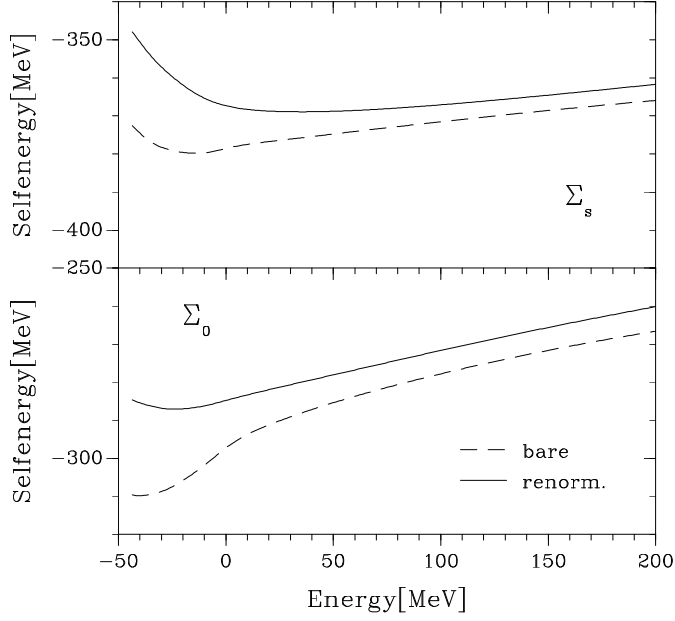


Figure 6: The real parts of the bare scalar and vector components (Σ_{qp}^s and Σ_{qp}^0), represented by the dashed line, are compared to the real parts of \mathcal{V}^s and \mathcal{V}^0 , renormalized according to eq. (38).

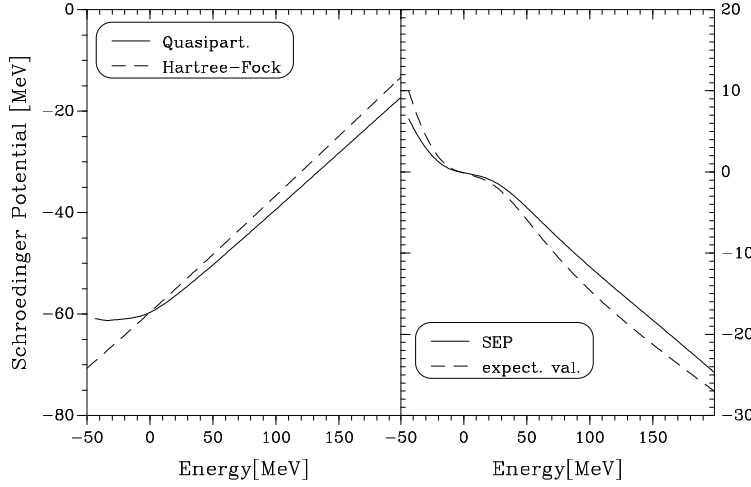


Figure 7: Energy dependence of the real (left) and imaginary part (right) of the Schrödinger equivalent potential. The result for the real part is compared to the corresponding prediction obtained in the HF approximation. The dashed curve in the right part of the figure exhibits the expectation value of W calculated according to (40).

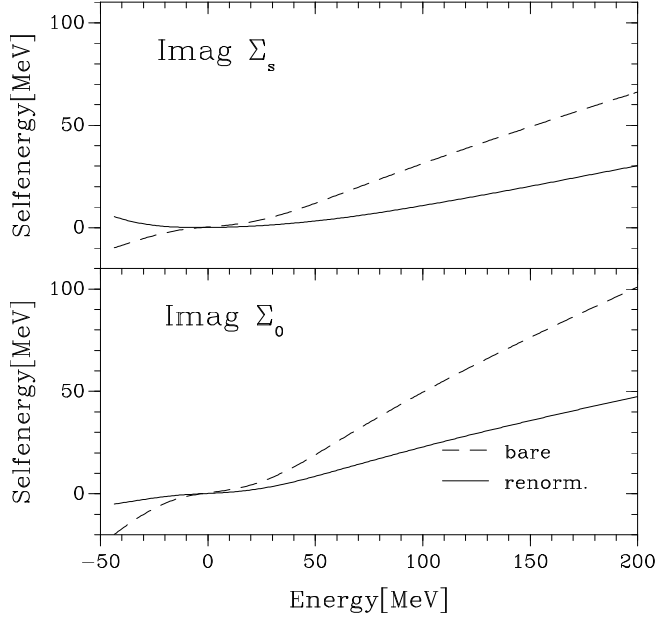


Figure 8: Bare and renormalized scalar and vector components of the imaginary part of the quasiparticle self-energy. For further details see Fig. 6.

2h1p terms, exhibit a dependence on the quasiparticle energy, which is very similar to the one derived from the HF approximation. Therefore one may conclude that the energy-dependence in the depth of central, Woods-Saxon type, optical potentials, used to describe nucleon-nucleus scattering is mainly due to the relativistic structure of the underlying Hartree-Fock self-energy to be used in a Dirac equation. Dispersive effects due to the consideration of 2p1h and 2h1p terms also lead to an energy dependence, which, however, is much smaller. These dispersive corrections tend to make the potential slightly more attractive at higher energies. It should be mentioned, however, that an energy dependence of the central Schrödinger potential similar to the one obtained here within the relativistic scheme can also be obtained within a non-relativistic Hartree-Fock due to large non-localities in the Hartree-Fock potential[19].

An analysis rather similar to the one just outlined for the real components of the self-energy can also be performed for the imaginary parts. Results for the renormalized Dirac components $\mathcal{W}^\alpha = \text{Imag}\mathcal{V}^\alpha$ ($\alpha = s$ and 0) are presented in Fig. 8 and compared to the bare scalar- and vector imaginary components. As we discussed already in the beginning of this section, the imaginary part of the bare components are negative for energies below the Fermi energy (2h1p), zero around $\omega = 0$ (ϵ_F) and positive for positive energies (2p1h). The renormalizing effects of the space like vector components are much more important for the imaginary part than for the real part. This can be deduced from the differences between \mathcal{W}^α and W^α : the bare components are as large as twice the renormalized quantities.

The imaginary part of the Schrödinger optical potential [eq. (39)] is shown on the right of Fig. 7. An alternative way of evaluating this imaginary part would be to

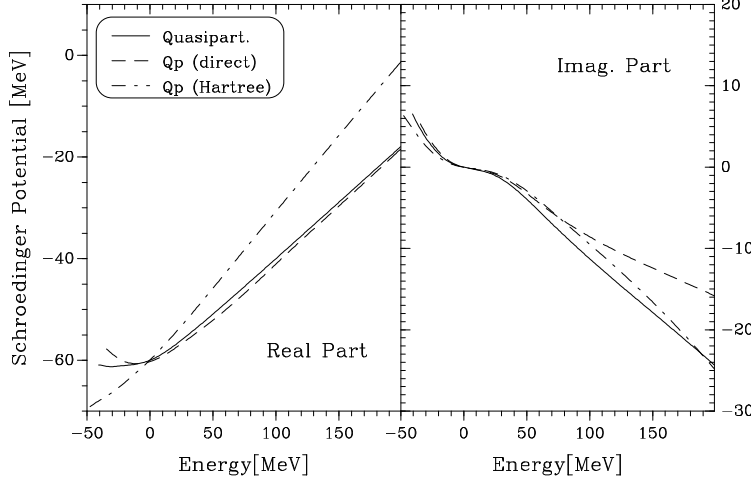


Figure 9: Real and Imaginary parts of the Schrödinger equivalent potential, calculated using the full model (solid lines), ignoring exchange diagrams in the evaluation of the terms of second order (dashed line), and using the Hartree approximation also for the lowest order term (dashed-dotted line)

calculate the expectation value of the Dirac operator

$$\bar{u}_{qp} \left[W^s - \gamma^0 W^0 + \boldsymbol{\gamma} \cdot \mathbf{k} W^v \right] u_{qp} \quad (40)$$

using the quasiparticle Dirac spinors of (33). These expectation values lead to the dashed line on the right part of Fig. 7. We see that the results for the imaginary part of the Schrödinger potential are rather insensitive on the way of calculation.

In the calculation of the imaginary components of the self-energy discussed in section 2 and consequently also in the corresponding real components, we always determined the Direct- and Exchange-contributions (see eqs. (16) and (18)). In order to explore the importance of the 2p1h and 2h1p exchange terms we compare in Fig. 9 the results obtained for the real and imaginary part of the Schrödinger equivalent potential with (solid lines) and without (dashed lines) inclusion of the exchange terms in the 2p1h and 2h1p parts of the self-energy. One finds that the effects of the exchange terms on the real part are rather small typically around 1 MeV. However, the effects are significantly larger for the imaginary part where the difference gets as large as 30 percent of the total result. This can be understood from the fact that the real part of the self-energy is dominated by the Hartree-Fock contribution, which is identical in these two approaches.

If one ignores the exchange terms in calculating the 2p1h and 2h1p terms, one may consider it more consistent to ignore the exchange term also in the leading contribution and replace the Hartree-Fock approximation by the Hartree-approach. In ref.[7] effective meson-nucleon coupling constants were determined to reproduce the DBHF results within a Dirac-Hartree model. The resulting coupling constants are a bit larger than those derived from the Dirac-Hartree-Fock analysis. If we use these Hartree-coupling constants and ignore the effects of exchange terms in the leading term as well as in the 2p1h and 2h1p terms, one arrives at a Schrödinger equivalent potential displayed

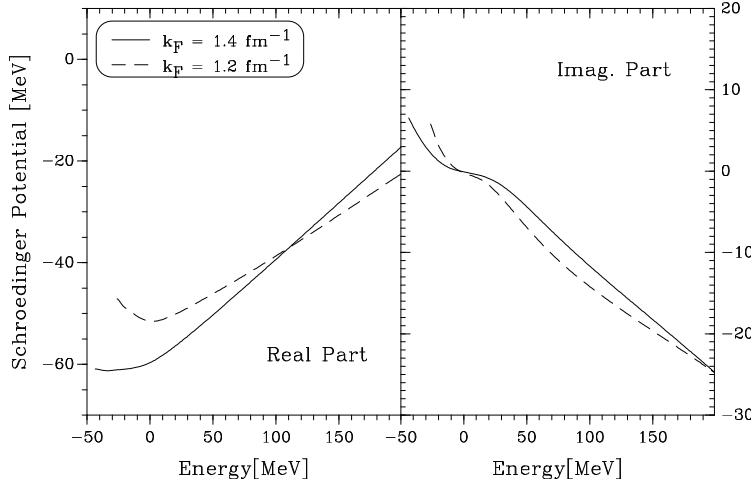


Figure 10: Real and Imaginary parts of the Schrödinger equivalent potential calculated for nuclear matter with a Fermi momentum of $k_F = 1.4 \text{ fm}^{-1}$ (solid line) are compared to those obtained for $k_F = 1.2 \text{ fm}^{-1}$.

by the dashed-dotted lines in Fig. 9. The differences to the solid lines get now quite pronounced for the real part. This can be traced back to the fact that in the Dirac-Hartree approximation Σ^s and Σ^0 are independent on the momentum or energy of the state and Σ^v is identical to zero. The results for the imaginary part obtained in this approach, however, are rather close to those evaluated with inclusion of the exchange contributions.

It is also interesting to investigate the density dependence of the self-energy in order to extend these calculations to finite nuclei. As an example we present some results obtained for nuclear matter with a Fermi momentum $k_F = 1.2 \text{ fm}^{-1}$ in Fig. 10. The results obtained at these various densities, either for the self-energy keeping track of the Dirac structure, or using the Schrödinger equivalent potentials derived from these components, may than be used in a local density approximation for a prediction of nucleon-nucleus scattering. Such investigations are in progress.

4 Conclusions

The relativistic structure of the self-energy for a nucleon in nuclear matter is investigated by including all irreducible terms of first and second order in the residual interaction. For the NN interaction a parameterization of the Dirac-Brueckner-Hartree-Fock (DBHF) G -matrix in terms of the exchange of effective scalar and vector mesons has been used. The 2p1h and 2h1p contributions to the imaginary part of the self-energy are evaluated keeping track of all direct and exchange terms. The corresponding 2p1h and 2h1p contributions to the real part are derived from these imaginary components by means of dispersion relations. A subtracted dispersion relation must be used for the 2p1h term to avoid double-counting with the G -matrix underlying the DBHF approach on which these studies are based.

The inclusion of 2h1p diagrams in the evaluation of the real part of the self-energy

yields a non-negligible modification of the scalar and vector components in particular for states with momenta below the Fermi momentum. Also the value of the quasiparticle energy is increased by a value as large as 17.5 MeV for momenta close to zero and to values around 5.3 MeV for $k = k_F$. Such a large effect for the quasiparticle energy may indicate that the 2h1p terms should have some effect in the calculation of the total energy.

The calculated self-energy can also be transformed into a Schrödinger equivalent optical potential, to be used in the study of nucleon-nucleus scattering. Exchange diagrams are non-negligible in the evaluation of the imaginary part. The energy- or momentum-dependence of the central component of the real potential, however, is dominated by the effects of the Dirac-Hartree-Fock contribution. The 2p1h and 2h1p terms give rise to a more attractive SEP at positive energies and introduce an additional energy dependence which is very weak.

This project has been supported by the Spanish research grant DGICYT, PB95-1249, and by the EC contract CHRX-CT93-0323. One of us (H.M.) is pleased to acknowledge the warm hospitality at the Facultat de Física, Universitat de Barcelona, and the support from the program of visiting Professor at this University.

References

- [1] J.D. Walecka and B.D. Serot, *Adv. Nucl. Phys.* **16**
- [2] R. Machleidt, *Adv. Nucl. Phys.* **19** (1989), 189
- [3] R. Brockmann and R. Machleidt, *Phys. Rev. C* **42** (1990), 1965
- [4] B. ter Haar and R. Malfliet, *Phys. Rep.* **149** (1987), 207
- [5] F. Coester, S. Cohen, B.D. Day, and C.M. Vincent, *Phys. Rev. C* **1** (1970), 769
- [6] K.W. Schmid, H. Müther, and R. Machleidt, *Nucl. Phys. A* **530** (1991), 14
- [7] R. Fritz and H. Müther, *Phys. Rev. C* **49** (1994), 633
- [8] F. Boersma and R. Malfliet, *Phys. Rev. C* **49** (1994), 1495
- [9] H. Müther and L.D. Skouras, *Nucl. Phys. A* **581** (1995), 247
- [10] M.F. Jiang, T.T.S. Kuo, and R. Machleidt, *Phys. Rev. C* **43** (1991), 1469
- [11] M.F. Jiang, T.T.S. Kuo, and H. Müther, *Phys. Rev. C* **38** (1988), 240
- [12] C. J. Horowitz, *Nucl. Phys. A* **412** (1984), 228
- [13] S. A. Chin, *Ann. Phys.* **108** (1977), 301
- [14] M. H. Steffani, M. Betz, and Th. A. J. Maris, *Nucl. Phys. A* **493** (1989), 493
- [15] Y.L. Han, Q.B. Shen, Y.Z. Zhuo, and T.M. Geng, *Nucl. Phys. A* **569** (1994), 732

- [16] H. Elsenhans and H. Mütter, *Nucl. Phys.* **A515** (1990), 715
- [17] W.H. Dickhoff and H. Mütter, *Rep. Prog. in Phys.* **11** (1992), 1947
- [18] T. Mitsumori, N. Noda, K. Koide, H. Kouno, A. Hasegawa, and M. Nakano, *Prog. Theoret. Phys.* **96** (1996), 179
- [19] M. Kleinmann, R. Fritz, A. Ramos, and H. Mütter, *Nucl. Phys.* **A 579** (1994), 85